SPANDIDOS PUBLICATIONS

ONCOLOGY REPORTS 46: 127, 2021

MicroRNA-454-5p promotes breast cancer progression by inducing epithelial-mesenchymal transition via targeting the FoxJ2/E-cadherin axis

CUI-PING WANG[1*], YONG-ZHENG YU[1*], HUI ZHAO[1], LI-JUAN XIE[2], QI-TANG WANG[1], YE WANG[3] and QIANG MU[1]

[1]The First Department of Breast Surgery, Qingdao Central Hospital, The Second Affiliated Hospital of Medical College of Qingdao University, Qingdao, Shandong 266042; [2]Department of Ophthalmology, Qingdao Women and Children's Hospital, Qingdao University, Qingdao, Shandong 266034; [3]Clinical Laboratory, Qingdao Central Hospital, The Second Affiliated Hospital of Medical College of Qingdao University, Qingdao, Shandong 266042, P.R. China

Received September 6, 2020; Accepted March 3, 2021

DOI: 10.3892/or.2021.8078

Abstract. MicroRNAs are important for the regulation of multiple cellular functions and are involved in the initiation and progression of various types of cancer, including breast cancer. Although microRNA (miR)-454-3p is reported to function as an oncogene in several types of human cancer, the role of miR-454-5p in breast cancer remains unknown. The present study demonstrated that miR-454-5p was upregulated in breast cancer and was associated with a poor prognosis in patients with breast cancer. Overexpression of miR-454-5p promoted breast cancer cell viability, migration and invasion *in vitro*, whereas silencing of miR-454-5p inhibited breast cancer proliferation, migration and invasion *in vitro* and suppressed tumor growth *in vivo*. Mechanistically, forkhead box J2 (FoxJ2) was shown to be a target of miR-454-5p and transactivated E-cadherin expression. Moreover, silencing of miR-454-5p reversed the epithelial-mesenchymal transition phenotype through upregulation of the FoxJ2/E-cadherin axis. Collectively, the present findings suggested that miR-454-5p may serve as a novel therapeutic target and prognostic predictor for patients with breast cancer.

Correspondence to: Dr Qiang Mu, The First Department of Breast Surgery, Qingdao Central Hospital, The Second Affiliated Hospital of Medical College of Qingdao University, 127 Si-Liu-Nan Road, Qingdao, Shandong 266042, P.R. China
E-mail: muqiangzhxyy@163.com

[*]Contributed equally

Key words: microRNA-454-5p, forkhead box J2, E-cadherin, epithelial-mesenchymal transition, migration and invasion, breast cancer

Introduction

Breast cancer is one of the most commonly diagnosed cancer types and the second leading cause of cancer-related mortality in women world-wide (1,2). Although early detection and systemic therapy significantly improve the outcome of patients with breast cancer, the survival rate of patients with metastatic breast cancer remains relatively low, with a 5-year survival of <25% (3,4). Therefore, it is important to understand the underlying molecular mechanism of breast carcinogenesis and progression, as well as to identify novel biomarkers and therapeutic target molecules for early diagnosis and individualized therapy.

MicroRNAs (miRNAs) are endogenous small non-coding RNAs, ~22 nucleotides in length, that are involved in gene silencing through translational repression or mRNA degradation by binding to the 3'-untranslated regions (3'-UTRs) of target genes (5). Previous studies have reported that miRNAs participate in multiple biological functions and are involved in various physiological processes, including cell proliferation, differentiation, metabolism, senescence and apoptosis (6,7). Aberrant expression of miRNAs has been shown to be involved in the development and progression of multiple human cancer types (8). In humans, miRNA (miR)-454 is located on chromosome 17q22, and it has two main mature forms: miR-454-5p and miR-454-3p. miR-454 has been identified as either an oncogene or a tumor suppressor in various types of cancer, including pancreatic cancer (9,10), colon cancer (11), melanoma (12), chondrosarcoma (13), glioma (14-16), hepatocellular carcinoma (17,18), lung cancer (19-21), laryngeal cancer (22), ovarian cancer (23), prostate cancer (24), gastric cancer (25-28), cervical cancer (29), bladder cancer (30), oral squamous cell carcinoma (31), osteosarcoma (32), renal carcinoma (33) and breast cancer (34-36). Although several studies have reported that miR-454-3p could function as an oncogene in breast cancer, the role of miR-454-5p remains unknown.

Epithelial-mesenchymal transition (EMT) is a biological process through which epithelial cells lose cell polarity and cell-cell adhesion; cells also acquire a fibroblastic morphotype

with invasive and migratory properties during tissue fibrosis, embryonic development and cancer progression (37,38). EMT contributes to cancer progression, metastasis and therapeutic resistance in all types of human cancer, which may correlate with unfavorable outcomes of patients with cancer (39). Therefore, targeting components of EMT signaling is considered as a promising strategy in cancer therapy. Previous studies have shown that miRNAs participate in EMT regulation during breast cancer progression (40,41).

The present study aimed to investigate the role of miR-454-5p in breast cancer progression both *in vitro* and *in vivo*, and explored the potential mechanism of miR-454-5p on the regulation of EMT in breast cancer.

Materials and methods

Cell lines and culturing. The human breast epithelial cell line MCF10A and breast cancer cell lines MCF7, T47D, BT549, MDA-MB-231 and SKBR3 were obtained from The Cell Bank of Type Culture Collection of The Chinese Academy of Sciences. MCF10A cells were cultured in DMEM/F12 (Hyclone; Cytiva) supplemented with 5% horse serum (Thermo Fisher Scientific, Inc.), 10 μg/ml insulin (Sigma-Aldrich; Merck KGaA), 20 ng/ml epidermal growth factor (R&D Systems, Inc.), 0.1 μg/ml cholera toxin (Sigma-Aldrich; Merck KGaA) and 0.5 μg/ml hydrocortisone (Sigma-Aldrich; Merck KGaA). BT549, MDA-MB-231 and SKBR3 cells were maintained in RPMI-1640 (Hyclone; Cytiva) supplemented with 10% FBS (Thermo Fisher Scientific, Inc.). MCF7 and T47D cells were cultured in DMEM (Hyclone; Cytiva) with 10% FBS. All cells were supplemented with 100 mg/ml streptomycin (Hyclone; Cytiva) and 100 IU/ml penicillin (Hyclone; Cytiva) and cultured in an atmosphere containing 5% CO_2 at 37˚C.

Transfections. miR-454-5p mimics (5'-GAAGUAAAGGGG CAAGAUAGGGC-3') and negative control (5'-UUCUCCGAA CGUGUCACGUUU-3') oligonucleotides were purchased from Guangzhou RiboBio Co., Ltd. Transient transfection was conducted using Lipofectamine® 3000 (Thermo Fisher Scientific, Inc.) according to the manufacturer's instructions. Cell were seeded in a 6-well plate at a density of $2x10^5$ cells/well and then transfected with 200 pmol oligonucleotides at 37˚C for 24 h. Experiments were performed 48 h after transfection.

The miR-454-5p antisense strand (5'-GCCCUAUCU UGCCCCUUUACUUC-3') or inhibitor control (5'-UCU ACUCUUUCUAGGAGGUUGUGA-3'; anti-Control) was cloned into the pEZX-AM04 lentiviral vector (GeneCopoeia, Inc.) and short hairpin RNA (sh)FoxJ2 (5'-GCAAGCCACGATACAGCTATT-3') or shControl (5'-CCTAAGGTTAAGTCGCCCTCG-3') was cloned into the pLKO.1 lentiviral vector (GeneCopoeia, Inc.). 293T cells were transfected with 10 μg lentiviral vectors and 10 μg packaging vectors when the density of cells reached 80-90%. After transfection for 48 h at 37˚C, supernatants containing virus particles were harvested and purified. The lentiviral particles were used to infect targeted cells at 60% confluency with a multiplicity of infection of 30 and stable cells were selected with 800 mg/ml puromycin. The FoxJ2 knockdown efficiencies were confirmed by reverse transcription-quantitative PCR (RT-qPCR) and western blotting (Fig. S1).

RT-qPCR. Total RNA was extracted from breast cancer cells using TRIzol® reagent (Invitrogen; Thermo Fisher Scientific, Inc.) according to the manufacturer's protocol. The isolated RNA was reverse transcribed into cDNA using a PrimeScript™ RT Master Mix kit (Takara Biotechnology Co., Ltd.) according to the manufacturer's protocol. qPCR analysis was performed using SYBR Green Mix (Takara Biotechnology Co., Ltd.) on a CFX96 Touch™ Real-time PCR System (Bio-Rad Laboratories, Inc.); the thermocycling conditions were as follows: Initial denaturation for 8 min at 95˚C; followed by 40 cycles of two-step PCR at 95˚C for 20 sec and 60˚C for 1 min. The expression of mRNA or miRNA was normalized to GAPDH or U6, respectively. Data were analyzed using the $2^{-\Delta\Delta Cq}$ method (42). The qPCR primers are listed in Table I.

Western blotting. Total protein was isolated from cells using RIPA lysis buffer containing PMSF (both from Cell Signaling Technology, Inc.). Protein concentrations were determined using a BCA Protein Assay kit (Thermo Fisher Scientific, Inc.). All samples (40 μg per lane) were separated by SDS-PAGE on 10% gels and then transferred to polyvinylidene fluoride membranes (EMD Millipore). After blocking with 5% skimmed milk for 1 h at room temperature, the membrane was incubated with primary antibodies overnight at 4˚C, followed by washing with PBS and incubation with horseradish peroxidase-conjugated goat anti-rabbit (cat. no. 7074) or horse anti-mouse (cat. no. 7076) (both at a dilution of 1:2,000; Cell Signaling Technology, Inc.) secondary antibodies for 1 h at room temperature. The bands were visualized with ECL reagent (EMD Millipore). Antibodies against N-cadherin (cat. no. sc-393933), E-cadherin (cat. no. sc-71008), Vimentin (cat. no. sc-80975), FoxJ2 (cat. no. sc-514265) (all from Santa Cruz Biotechnology, Inc.) and GAPDH (cat. no. 5174; Cell Signaling Technology, Inc.) were used at a dilution of 1:1,000.

Luciferase reporter assay. For FoxJ2 3'-UTR activity analysis, the 3'-UTR of FoxJ2 mRNA and the corresponding sequence with mutations (FoxJ2-1: 5'-GCTGGCAAAGAAATGGAT AGGGA-3' to 5'-GCTGGCAAAGAAATGGATAAAA-3'; FoxJ2-2: 5'-GAAGTAAAGGGGCAAGATAGGGC-3' to 5'-GAAGTAAAGGGGCAAGATAAAAC-3') were cloned into a psiCHEK2 luciferase reporter plasmid (Promega Corporation). MDA-MB-231 cells were seeded into a 24-well plate at $1x10^4$ cells/well and co-transfected with psiCHEK2-FoxJ2 (500 ng) and miR-454-5p mimics (50 pmol) or negative control using Lipofectamine 3000 for 48 h at 37˚C. For E-cadherin promoter activity analysis, the E-cadherin promoter was cloned into a pGL3-basic luciferase reporter plasmid (Promega Corporation) and was transfected into MDA-MB-231 cells stably expressing anti-miR-454-5p or shFoxJ2, as well as into the control cells using Lipofectamine 3000 for 48 h at 37˚C. Luciferase activity was analyzed after transfection for 48 h and the cell lysates were measured for luciferase activity using Dual-Luciferase Reporter Assay System (Promega Corporation) according to the manufacturer's instructions. The firefly luciferase activity was normalized to *Renilla* luciferase activity.

Chromatin immunoprecipitation (ChIP) assay. Stably transfected MDA-MB-231 cells were cross-linked with 1% formaldehyde for 15 min at room temperature. After quenching

with 125 mM glycine, the cells were collected, washed and sonicated in RIPA buffer. The cross-linked lysate was sonicated (power, 20 W; duration, 30 sec/cycle for 40 cycles; temperature, 5-6˚C) to obtain 500-1,500 bp fragments, which were immunoprecipitated with IgG or anti-FoxJ2 antibody (cat. no. sc-514265; Santa Cruz Biotechnology, Inc.) at 4˚C for 3 h. This was followed by incubation with 50 μl protein A/G beads overnight at 4˚C. qPCR was used to identify and quantify the precipitated DNA. Primers for ChIP assays are presented in Table I.

Colony formation assay. Breast cancer cells were seeded into six-well plates at 500 cells/well. Transient transfection with miR-454-5p mimics was conducted using Lipofectamine® 3000, aforementioned, or MDA-MB-231 cells stably expressing anti-miR-454-5p or shFoxJ2 were used, as well as their control cells. Cells were cultured for 20 days at 37˚C, and colonies were washed with PBS, fixed with 4% paraformaldehyde for 15 min at room temperature, and stained with hematoxylin. The colonies with >50 cells were counted under a light microscope at x100 magnification.

Cell morphology. MDA-MB-231 cells stably expressing anti-miR-454-5p or shFoxJ2, as well as their control cells, were seeded in 6-well plates at a density of $5x10^4$ cells/well and cultured at 37˚C for 24 h. Cell morphology was examined under a light microscope at x100 magnification.

Cell viability assay. The Cell Counting Kit-8 (CCK-8; Dojindo Molecular Technologies, Inc.) was used to determine cell viability, according to the manufacturer's protocols. Cells were seeded into a 96-well plate at $5x10^3$ cells/well. After transfection for 24 h, CCK-8 reagent (10 μl) was added to the medium and incubated at 37˚C for 2 h. The absorbance of each sample was measured using a microplate reader (Thermo Fisher Scientific, Inc.) at 450 nm.

Immunofluorescence. Cells were plated at a density of $2x10^4$ on glass coverslips, washed with ice-cold PBS and fixed in 4% formaldehyde solution for 15 min at room temperature. The coverslips were blocked with 2% BSA (Cell Signaling Technology, Inc.) in PBS for 30 min at room temperature and incubated with a primary antibody against E-cadherin (1:500; cat. no. sc-71008; Santa Cruz Biotechnology, Inc.) overnight at 4˚C. Subsequently, cells were incubated with Alexa Fluor® 488-conjugated anti-mouse secondary antibody (1:300; cat. no. 4408; Cell Signaling Technology, Inc.) for 1 h and then stained with DAPI for 10 min, both at room temperature. The coverslips were washed with PBS and observed under a fluorescence microscope at x400 magnification.

Cell cycle analysis. Cells were seeded into a 6-well plate at a density of $5x10^4$ cells/well. After culture at 37˚C for 24 h, cells were collected and fixed with 70% ethanol for 24 h at -20˚C, followed by incubation with 10 μg/ml PI and 50 μg/ml RNase (BD Biosciences) on ice for 15 min. Cells were then assessed by flow cytometry using a BD FACSCalibur flow cytometer (BD Biosciences).

Transwell assays. Cell invasion and migration were assessed using BD Transwell chambers pre-coated with or without Matrigel, respectively (BD Biosciences). Cells were seeded ($2x10^4$ cells/well) into the upper Transwell chamber containing RPMI-1640 medium without serum; RPMI-1640 medium with 10% FBS was added to the bottom chamber. After incubation for 16 h at 37˚C, the invaded or migrated cells on the lower surface were fixed in 4% formaldehyde solution for 15 min at room temperature, and subsequently stained with crystal violet for 15 min at room temperature. Images of the invaded or migrated cells were captured under a light microscope at x100 magnification.

Table I. Primer sequences used in quantitative PCR.

Name	Primer sequence (5'→3')
FoxJ2	F: ATGGCTTCTGACCTAGAGAGTAG
	R: CTGCCTCGTCTTTGCTCAGG
E-cadherin	F: CGAGAGCTACACGTTCACGG
	R: GGGTGTCGAGGGAAAAATAGG
GAPDH	F: ATGACCCCTTCATTGACCTCA
	R: GAGATGATGACCCTTTTGGCT
E-cadherin R1	F: CTGTACAGAGCATTTATGGCTCAA
	R: TGTCTCCCTATGCTGTTGTGG
E-cadherin R2	F: GAGTCTCTTGAACCCGGCA
	R: CCACTGAGCTAGCAGCCTAAT
E-cadherin R3	F: CACTCCAGCTTGGGTGAAAGA
	R: GGCTCACTAAGACCTGGGAT

F, forward; FoxJ2, forkhead box J2; R, reverse; R1/R2/R3, region 1/2/3.

Bioinformatics analysis. TargetScan Human release 7.2. (http://www.targetscan.org) was used for prediction of miR-454-5p targets. The top three genes containing two potential miR-454-5p target sites were selected for further study. LASAGNA-Search 2.0 (https://www.bitnos.com/info/lasagna-search) was used to predict FoxJ2 binding sites on the E-cadherin promoter region.

Validation of gene expression and outcome by TCGA database. The expression levels of miR-454-5p were analyzed in breast cancer tissues (n=749) and normal breast tissues (n=76) obtained from The Cancer Genome Atlas (TCGA) database by using UALCAN (http://ualcan.path.uab.edu/index.html). The relationship between miR-454-5p and FoxJ2 was determined by ENCORI (http://starbase.sysu.edu.cn). The prognostic value of miR-454-5p expression was examined by using the online database, KM-Plotter (www.kmplot.com/mirpower). Patients were divided into two groups by 'auto select best cutoff' feature and assessed using a Kaplan-Meier survival plot.

Xenografts. Female BALB/c-nude mice (n=12; age, 5 weeks; weight, 22 g) were purchased from Vital River Lab Animal Technology Company. The mice were maintained in a specific pathogen-free environment with a 10/14-h light/dark cycle in 40-60% humidity at 27˚C and had *ad libitum* access to food and water. The experimental procedures were approved by

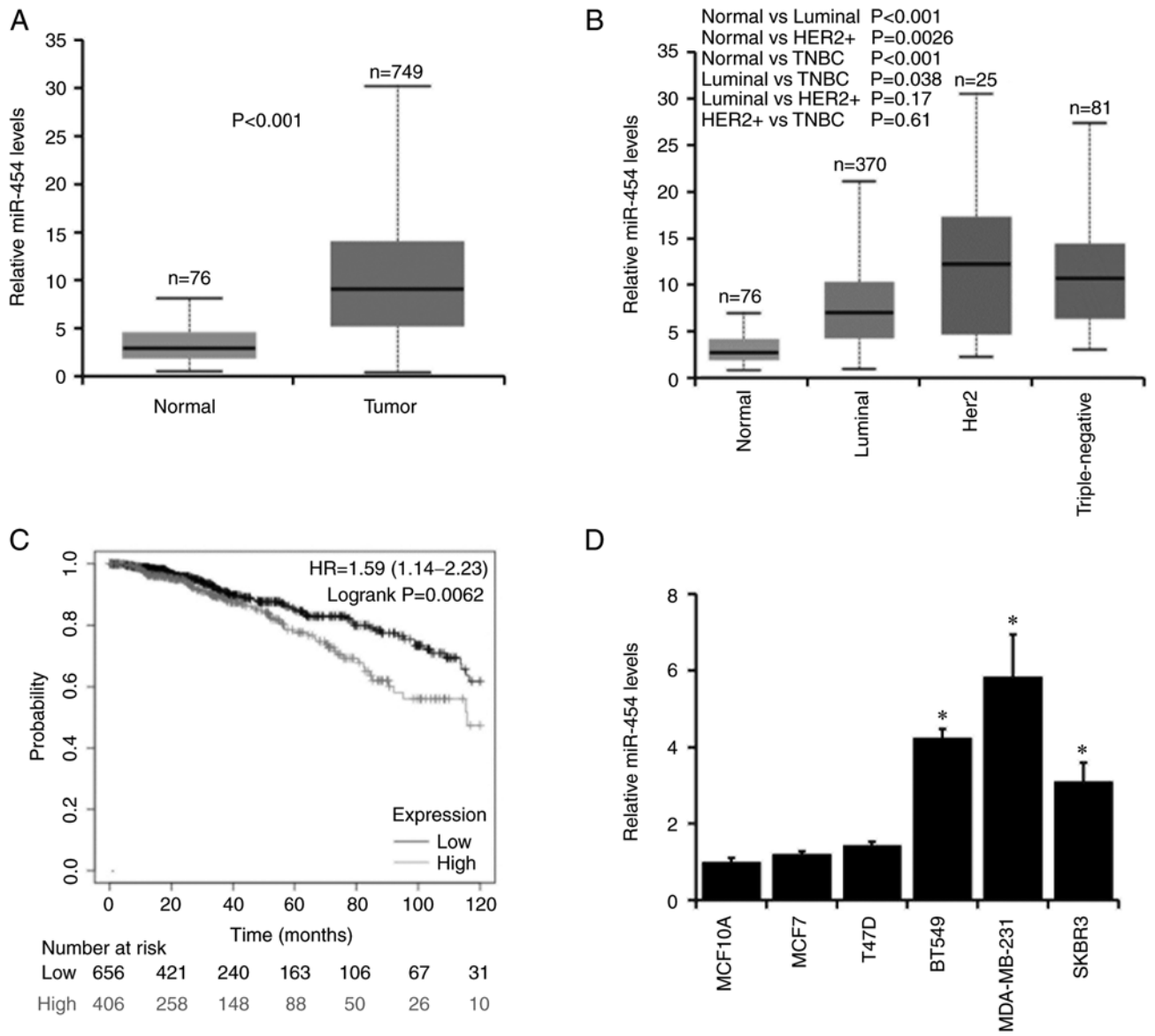

Figure 1. miR-454-5p expression is upregulated breast cancer. (A) Expression levels of miR-454-5p in breast cancer and normal tissue samples from The Cancer Genome Atlas database were analyzed. (B) Expression levels of miR-454-5p in different molecular subtypes of breast cancer and normal tissue samples analyzed in TCGA database by using UALCAN. (C) Overall survival of patients with different miR-454-5p expression levels, as evaluated using Kaplan-Meier Plotter. (D) Expression levels of miR-454-5p in five breast cancer cell lines and the normal breast epithelial cell line MCF10A were examined using reverse transcription-quantitative PCR. *P<0.05 vs. MCF10A. HR, hazard ratio; miR, microRNA.

the Animal Experimentation Ethics Committee of Qingdao Central Hospital (Qingdao, China). A total of $1x10^6$ stably transfected MDA-MB-231 cells were injected subcutaneously into the right mammary fat pad. Tumor volume was calculated using the following equation: (Length x $width^2$)/2. The mice were sacrificed on day 35 after tumor implantation, and the tumors were excised and weighed. The tumor burden did not exceed the recommended dimensions (tumor $diameter_{max}$ ≤16.5 mm; $volume_{max}$ ≤1,200 mm^3). The animals were anesthetized (60 mg/kg ketamine and 5.0 mg/kg xylazine) and then sacrificed by cervical dislocation.

Statistical analysis. Statistical analyses were performed using SPSS 20.0 (IBM Corp.). Data are presented as the mean ± SD from at least three independent experiments. The unpaired Student's t-test was used to compare differences between two groups, and one-way ANOVA followed by Tukey's multiple comparison post hoc test was used when comparing >2 groups. P<0.05 was considered to indicate a statistically significant difference.

Results

miR-454-5p is upregulated in breast cancer and is associated with poor prognosis. To determine the role of miR-454-5p in breast cancer, the expression levels of miR-454-5p were analyzed in breast cancer tissues (n=749) and normal breast tissues (n=76) obtained from The Cancer Genome Atlas (TCGA) database by using UALCAN. Increased miR-454-5p expression levels were observed in breast cancer compared with normal tissues (Fig. 1A), and miR-454-5p expression was significantly upregulated in triple-negative and $Her2^+$ breast

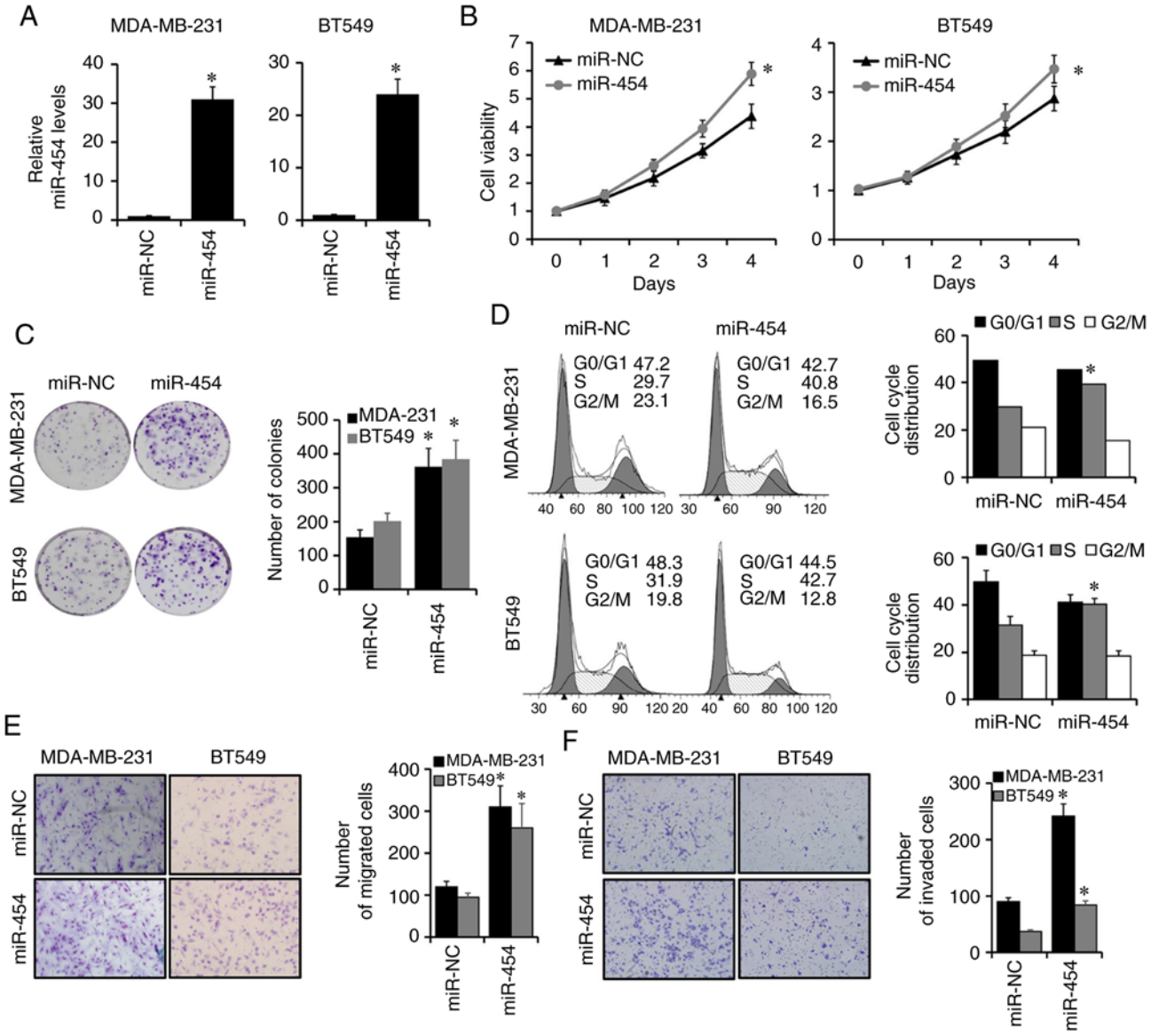

Figure 2. Overexpression of miR-454-5p promotes breast cancer cell proliferation, migration and invasion. (A) Expression levels of miR-454-5p in MDA-MB-231 and BT549 cells transfected with miR-454-5p mimics or negative control were determined using reverse transcription-quantitative PCR. (B) Cell viability in MDA-MB-231 and BT549 cells transfected with miR-454-5p mimics or negative control was assessed using a Cell Counting Kit-8 assay. (C) Colony formation analysis of MDA-MB-231 and BT549 cells transfected with miR-454-5p mimics or negative control. (D) Cell cycle analysis of MDA-MB-231 and BT549 cells transfected with miR-454-5p mimics or negative control. (E) Migration and (F) invasion analysis of MDA-MB-231 and BT549 cells transfected with miR-454-5p mimics or negative control was assessed by Transwell analyses. *P<0.05 vs. miR-NC. miR, microRNA; NC, negative control.

cancer types (Fig. 1B). Furthermore, high miR-454-5p expression was associated with a poor prognosis in patients with breast cancer as determined using the KM-Plotter database (Fig. 1C). Subsequently, the expression levels of miR-454-5p were examined in five breast cancer cell lines (MCF7, T47D, BT549, MDA-MB-231 and SKBR3) and a normal breast epithelial cell line MCF10A. The expression levels of miR-454-5p were significantly higher in BT549, MDA-MB-231 and SKBR3 breast cancer cell lines compared with MCF10A cells (Fig. 1D). Taken together, these results indicated that miR-454-5p may serve an important role in breast cancer progression.

Overexpression of miR-454-5p promotes breast cancer cell proliferation, migration and invasion. As miR-454-5p was upregulated in BT549, MDA-MB-231 and SKBR3 compared to MCF10A cells, aforementioned, which suggested that miR-454-5p may serve an important role in these cell lines, MDA-MB-231 and BT549 were choose to further study. To evaluate the potential role of miR-454-5p in breast cancer progression, miR-454-5p mimics or negative controls were transfected into MDA-MB-231 and BT549 cells. The expression of miR-454-5p was effectively elevated in MDA-MB-231 and BT549 cells after transfection with miR-454-5p mimics compared with miR-NC-transfected cells, as determined by RT-qPCR (Fig. 2A). CCK-8 and colony formation assays were conducted to evaluate the effects of miR-454-5p on breast cancer proliferation. It was found that the overexpression of miR-454-5p significantly enhanced cell viability and the number of colonies in MDA-MB-231 and BT549 cells compared with the miR-NC group (Fig. 2B and C, respectively). Furthermore,

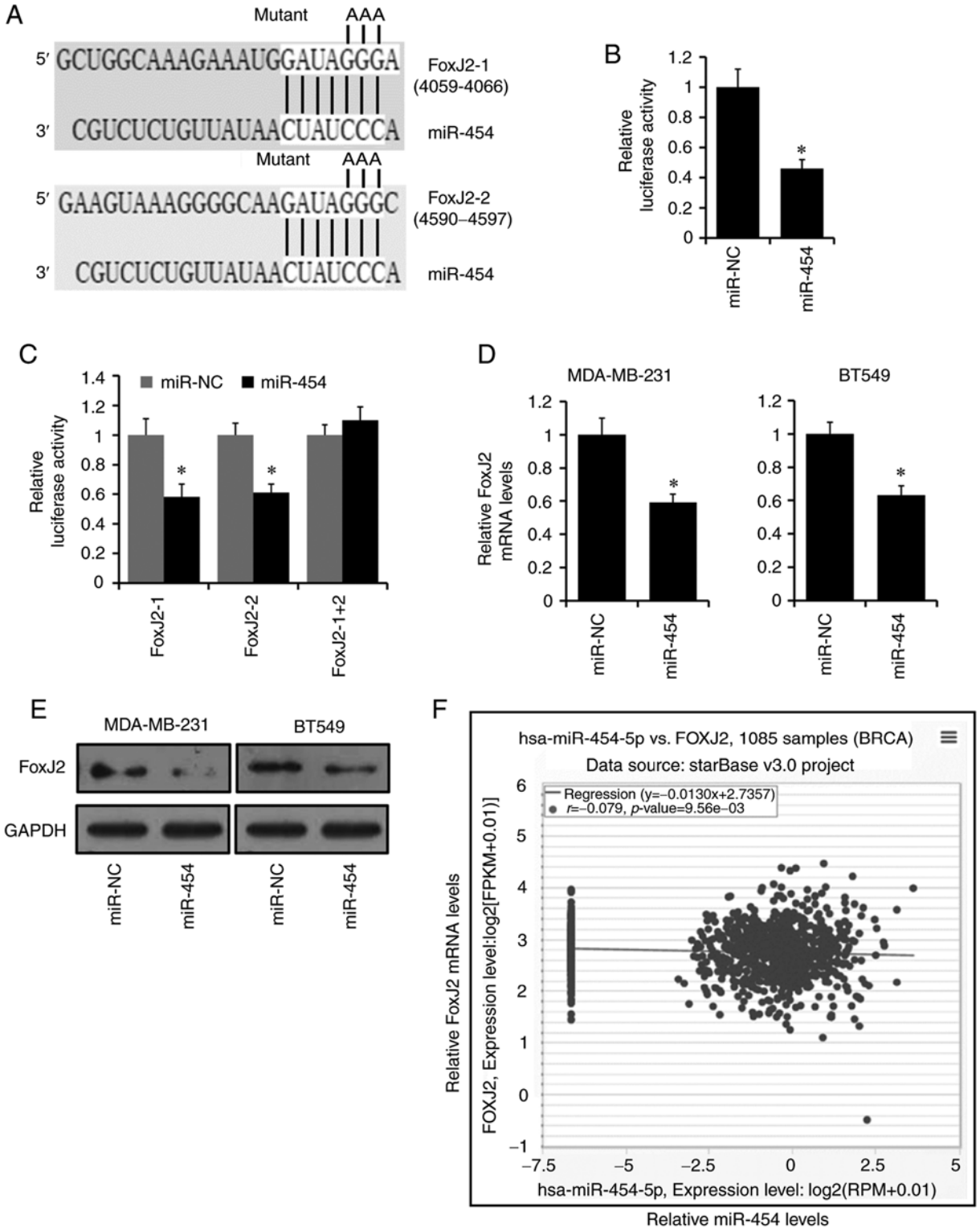

Figure 3. FoxJ2 is a target of miR-454-5p. (A) Schematic illustration of the two predicted miR-454-5p target sites in FoxJ2 3'-UTR. Luciferase reporter assays were performed to demonstrate that miR-454-5p inhibits the (B) wild-type but not the (C) double-mutant FoxJ2-1 + 2 3'-UTR target sites of FoxJ2 reporter activities. (D) mRNA and (E) protein expression levels of FoxJ2 in MDA-MB-231 or BT549 cells transfected with miR-454-5p mimics or negative control was examined using reverse transcription-quantitative PCR and western blotting, respectively. (F) Relationship between miR-454-5p and FoxJ2 expression levels analyzed by ENCORI. *P<0.05 vs. miR-NC. FoxJ2, forkhead box J2; miR, microRNA; UTR, untranslated region.

the proportion of cells at the S phase was significantly increased in miR-454-5p-overexpressing MDA-MB-231 and BT549 cells compared with that of control cells (Fig. 2D). Transwell analyses were performed to assess the effects of miR-454-5p on breast cancer cell migration and invasion (Fig. 2E and F, respectively). The number of migrated and invaded cells was significantly increased in miR-454-5p-overexpressing MDA-MB-231 and BT549 cells compared with those in control cells. These results suggested that miR-454-5p may function as an oncogene in breast cancer progression.

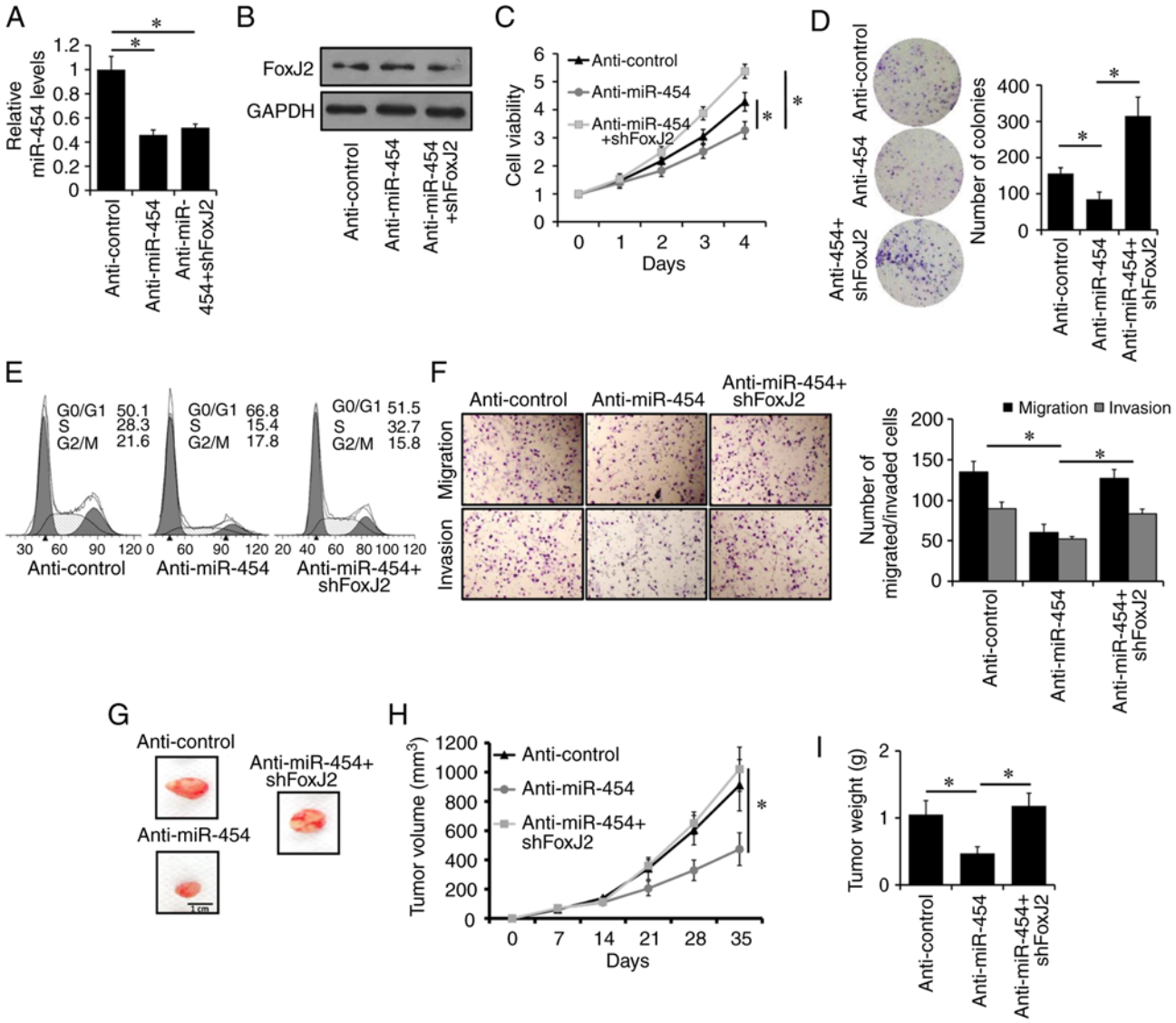

Figure 4. Silencing of miR-454-5p inhibits breast cancer progression through the upregulation of FoxJ2. Expression levels of (A) miR-454-5p and (B) FoxJ2 protein in MDA-MB-231 cells stably expressing anti-miR-454-5p with or without shFoxJ2 transfection, or anti-Control cells, were examined by reverse transcription-quantitative PCR or western blotting, respectively. (C) Cell viability and (D) colony formation in MDA-MB-231 cells stably expressing anti-miR-454-5p with or without shFoxJ2 transfection, or anti-Control cells, was assessed using a Cell Counting Kit-8 assay or colony formation assay, respectively. (E) Cell cycle analysis of MDA-MB-231 cells stably expressing anti-miR-454-5p with or without shFoxJ2 transfection, or anti-Control cells. (F) Migration and invasion of MDA-MB-231 cells stably expressing anti-miR-454-5p with or without shFoxJ2 transfection, or anti-Control cells, was assessed by Transwell or Matrigel analysis, respectively. (G) Representative images of the tumors formed by MDA-MB-231 cells stably expressing anti-miR-454-5p with or without shFoxJ2 transfection, or anti-Control cells, at the time of harvest. Tumor (H) volume and (I) weight of xenografted mice injected with MDA-MB-231 cells stably expressing anti-miR-454-5p with or without shFoxJ2 transfection, or anti-Control cells, at the indicated times. *P<0.05. FoxJ2, forkhead box J2; miR, microRNA; sh, short hairpin RNA.

FoxJ2 is a target of miR-454-5p. TargetScan was used to predict target genes of miR-454-5p, and the top three genes containing two potential target sites in their 3'-UTRs were ATXN7L3B, RIPPLY3 and FoxJ2 (Fig. 3A). Of the three genes, only FoxJ2 has been reported to be involved in cancer progression (43-46); therefore, it was selected for further study. The luciferase reporter assay was used to determine whether miR-454-5p could directly bind to the 3'-UTR of FoxJ2. The two putative miR-454-5p target sites in the 3'-UTR of FoxJ2 were cloned into the psiCHEK2 reporter plasmid and subsequently transfected into MDA-MB-231 cells along with miR-454-5p mimics or negative control. The luciferase activity of the FoxJ2 3'-UTR reporter construct was significantly decreased in the miR-454-5p-transfected MDA-MB-231 cells compared with luciferase activity in the miR-NC cells (Fig. 3B). This effect was abolished in the mutated FoxJ2 3'-UTR group in which both target sites for miR-454-5p were inactivated (FoxJ-1 + 2) by site-directed mutagenesis (Fig. 3C). The expression levels of FoxJ2 were notably decreased in MDA-MB-231 and BT549 cells transfected with miR-454-5p mimics compared with the expression levels in control cells, as demonstrated by RT-qPCR (Fig. 3D) and western blotting (Fig. 3E).

To further investigate the relationship between miR-454-5p and FoxJ2, the expression levels of miR-454-5p and FoxJ2 from TCGA database was analyzed by ENCORI. As presented in Fig. 3F, the expression of miR-454-5p exhibited a negative

co-expression trend with FoxJ2. Thus, these results support the bioinformatics prediction that FoxJ2 was a direct target of miR-454-5p.

Silencing of miR-454-5p inhibits breast cancer proliferation, migration and invasion by upregulating FoxJ2 expression. To further confirm the regulation of the miR-454-5p/FoxJ2 axis in breast cancer progression, stably transfected MDA-MB-231 cell lines overexpressing the anti-miR-454-5p inhibitor with or without shFoxJ2 co-transfection, as well as anti-Control cells, were generated. The expression of miR-454-5p was significantly downregulated in miR-454-5p-silenced MDA-MB-231 cells compared with that of control cells, as determined via RT-qPCR (Fig. 4A). The expression of FoxJ2 was upregulated in miR-454-5p-silenced MDA-MB-231 cells, whereas it was notably downregulated in miR-454-5p and FoxJ2-silenced MDA-MB-231 cells compared with that of control cells, as determined using western blotting (Fig. 4B). It was also found that knockdown of FoxJ2 significantly reversed the inhibitory effects of miR-454-5p silencing on the proliferation, migration and invasion of MDA-MB-231 cells as determined via CCK-8 (Fig. 4C), colony formation (Fig. 4D), cell cycle (Fig. 4E) and Transwell assays (Fig. 4F), respectively.

To investigate the biological effect of the miR-454-5p/FoxJ2 axis on breast cancer progression *in vivo*, MDA-MB-231-control, MDA-MB-231-anti-454 and MDA-MB-231-anti-454 + shFoxJ2 cells were injected into the mammary fat pads of female BALB/c-nude mice. As presented in Fig. 4G-I, tumor volumes and weights were significantly decreased in mice injected with MDA-MB-231-anti-miR-454 cells compared with those in mice injected with MDA-MB-231-control cells. Moreover, it was identified that knockdown of FoxJ2 could abolish the inhibitory effects of miR-454-5p silencing on tumor growth. Collectively, these results indicated that silencing of miR-454-5p may inhibit breast cancer progression through the upregulation of FoxJ2 expression.

Silencing of miR-454-5p reverses EMT through the transcriptional upregulation of E-cadherin. Accumulating evidence has suggested that EMT could promote progression in breast cancer (41). Therefore, it was investigated whether miR-454-5p regulated EMT to affect breast cancer progression. It was identified that miR-454-5p-silenced MDA-MB-231 cells had a cobblestone-like morphology, whereas anti-miR-454-5p + shFoxJ2 MDA-MB-231 cells and anti-Control cells maintained their spindle-like fibroblast morphology (Fig. 5A). In addition, it was demonstrated that the expression of epithelial marker E-cadherin was increased in miR-454-5p-silenced MDA-MB-231 cells, whereas the expression levels of mesenchymal markers Vimentin and N-cadherin were decreased in miR-454-5p-silenced MDA-MB-231 cells compared with the expression levels in control cells, as determined by western blotting (Fig. 5B). Moreover, knockdown of FoxJ2 could reverse this effect caused by miR-454-5p silencing (Fig. 5B). In total, three putative FoxJ2 binding sites on the E-cadherin promoter region were identified using LASAGNA-Search (47). ChIP analysis results demonstrated that FoxJ2 bound to region 1 and region 2 from the E-cadherin promoter region (Fig. 5C). Luciferase assay results indicated that knockdown of FoxJ2 significantly abolished miR-454-5p depletion-induced E-cadherin promoter activity (Fig. 5D). E-cadherin mRNA expression levels were increased in miR-454-5p-silenced MDA-MB-231 cells, whereas this effect was abolished by FoxJ2 knockdown as shown by RT-qPCR (Fig. 5E) and immunofluorescence (Fig. 5F). E-cadherin mRNA was determined to be positive co-expression trend with FoxJ2 mRNA by ENCORI (Fig. 5G). Together, these results indicated that miR-454-5p may regulated EMT through the transcriptional upregulation of E-cadherin by FoxJ2.

Discussion

The results from present study demonstrated that miR-454-5p was upregulated in breast cancer compared with normal breast epithelial tissue and cell lines. Furthermore, the results suggested that miR-454-5p may promote breast cancer progression both *in vitro* and *in vivo*. FoxJ2 was identified as a direct target of miR-454-5p, and FoxJ2 may transactivate the expression of E-cadherin. Moreover, silencing of miR-454-5p reversed EMT through the transactivation of E-cadherin by FoxJ2. The present results suggested that miR-454-5p may be a potential target for breast cancer therapy.

Accumulating evidence has revealed that the dysregulation of miRNAs is involved in carcinogenesis and cancer progression in all types of human cancer, including breast cancer (41,48). Abnormal expression of miR-454 has been observed in a variety of human cancer types, suggesting that miR-454 may serve an important role in cancer development and progression (9-36). miR-454-3p has been demonstrated to function as an oncogene, and high expression of miR-454-3p may be associated with unfavorable outcome in triple-negative breast cancer (36,49). Moreover, miR-454-3p has been shown to promote breast cancer metastasis through the suppression of Wnt/β-catenin signaling antagonists (35). Consistent with these previous reports, the present study demonstrated that miR-454-5p was upregulated in breast cancer and that miR-454-5p may promote breast cancer progression both *in vitro* and *in vivo*, suggesting that miR-454-5p may function as an oncogene in breast cancer.

Fox protein family members share a highly conserved common forkhead DNA-binding domain and are widespread from yeast to humans (50). These transcription factors are crucial players in multiple cellular processes, including differentiation, proliferation, metabolism, migration and apoptosis, and are often dysregulated in cancer development and progression (50). FoxJ2 belongs to the human Fox gene family and serves an important role in embryogenesis and carcinogenesis (51). FoxJ2 has also been reported to function as a tumor suppressor in multiple types of cancer, including colorectal cancer (52), hepatocellular carcinoma (53), non-small lung cancer (43), extrahepatic cholangiocarcinoma (44), glioma (45) and breast cancer (46). In line with the aforementioned results, the present findings demonstrated that FoxJ2 was a target of miR-454-5p and that miR-454-5p may promote breast cancer progression through the downregulation of FoxJ2 expression.

EMT, a main driver of tumor metastasis, is defined as a process by which epithelial cells lose their cell polarity and

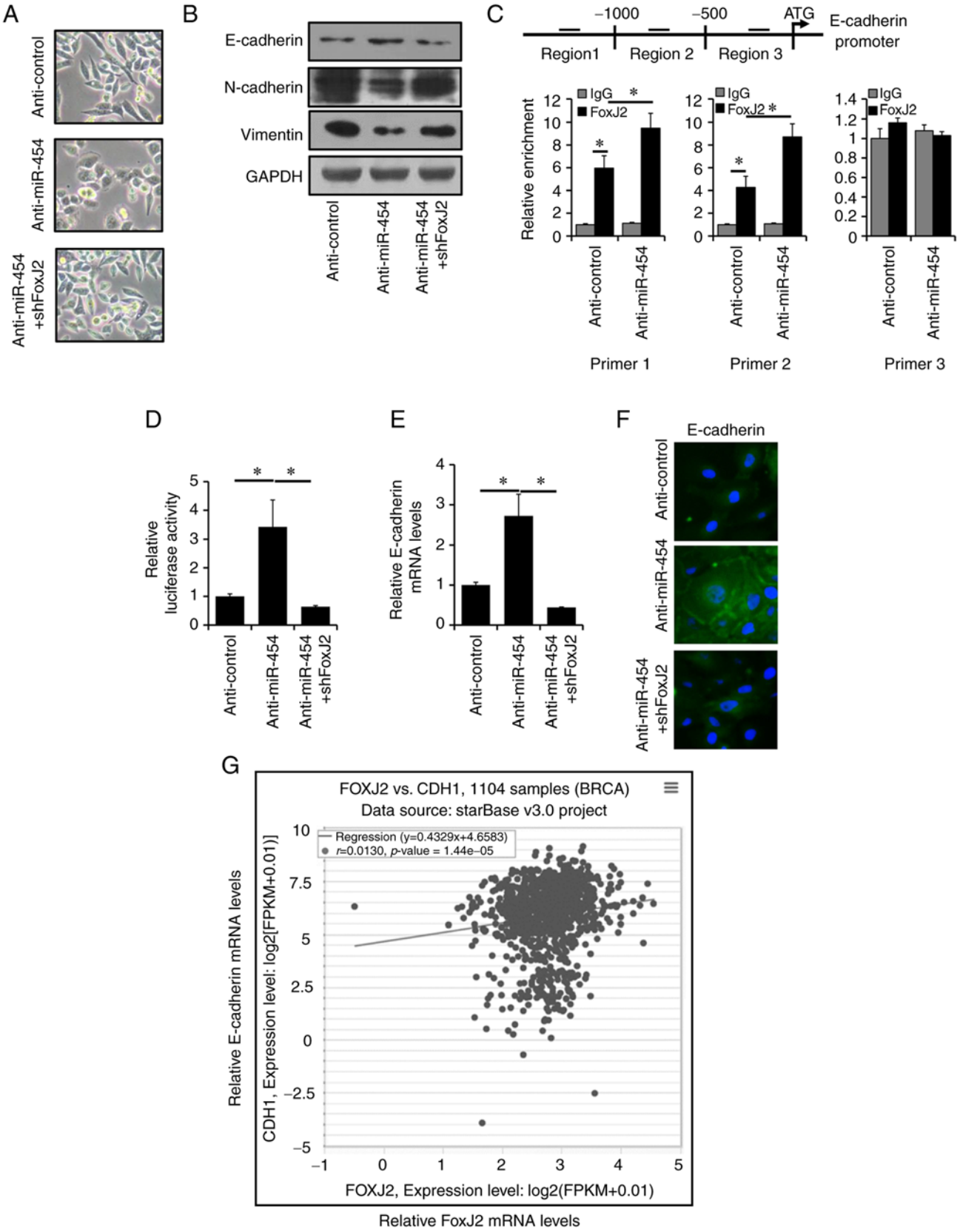

Figure 5. Silencing of miR-454-5p reverses EMT through the upregulation of the FoxJ2/E-cadherin axis in breast cancer. (A) Bright-field images of MDA-MB-231 cells stably expressing anti-miR-454-5p with or without shFOXJ2 co-transfection, and anti-Control cells. (B) Expression levels of E-cadherin, N-cadherin and Vimentin in cells stably expressing anti-miR-454-5p with or without shFOXJ2 co-transfection, and anti-Control cells were examined by western blotting. (C) Chromatin immunoprecipitation analysis of miR-454-5p-silenced MDA-MB-231 cells or anti-Control cells to determine the binding of FoxJ2 to three E-cadherin promoter regions. (D) Luciferase analysis of E-cadherin promoter activity in MDA-MB-231 cells stably expressing anti-miR-454-5p with or without shFOXJ2 co-transfection, and anti-Control cells. (E) mRNA expression level of E-cadherin in MDA-MB-231 cells stably expressing anti-miR-454-5p with or without shFOXJ2 co-transfection, and anti-Control cells was examined by reverse transcription-quantitative PCR. (F) Expression of E-cadherin in cells stably expressing anti-miR-454-5p with or without shFOXJ2 co-transfection, and anti-Control cells was examined using immunofluorescence. (G) Relationship between E-cadherin and FoxJ2 expression levels analyzed by ENCORI. *P<0.05. FoxJ2, forkhead box J2; miR, microRNA; sh, short hairpin RNA.

cell-cell adhesions, resulting in changes to cell morphology and enhanced cell migratory and invasive abilities (37). Vimentin, N-cadherin and E-cadherin are generally considered as EMT markers. During the EMT process, the expression of E-cadherin (an epithelial marker) is decreased, whereas the expression levels of Vimentin and N-cadherin (mesenchymal markers) are increased. Several studies have reported that FoxJ2 can inhibit cancer migration, invasion and the EMT phenotype (43-44,52,53). Consistent with these findings, the present study identified a decrease in Vimentin and N-cadherin expression levels, and an increase in E-cadherin expression in miR-454-5p-silenced cells, whereas knockdown of FoxJ2 reversed these effects, suggesting that miR-454-5p may induce an EMT phenotype in breast cancer. Furthermore, it was revealed that FoxJ2 could bind to the E-cadherin promoter region and transactivated E-cadherin expression. Thus, the present results suggested that miR-454-5p promoted breast cancer progression through the induction of an EMT phenotype by downregulating the FoxJ2/E-cadherin axis.

In conclusion, the present study demonstrated that miR-454-5p was upregulated in breast cancer. It was suggested that miR-454-5p may promote breast cancer progression through the induction of EMT by targeting the FoxJ2/E-cadherin axis. Therefore, miR-454-5p may serve as a novel therapeutic target and prognostic predictor for patients with breast cancer.

Acknowledgements

Not applicable.

Funding

Not applicable.

Availability of data and materials

The datasets used and/or analyzed during the present study are available from the corresponding author on reasonable request.

Authors' contributions

CPW and YZY contributed to writing the manuscript collection and analysis of data. HZ, LJX, YW, and QTW collected and interpreted data. QM contributed to study conception and design as well as revising and approving the final version of the manuscript. CPW and QM confirm the authenticity of all the raw data. All authors read and approved the final manuscript.

Ethics approval and consent to participate

The experimental procedures were approved by the Animal Experimentation Ethics Committee of Qingdao Central Hospital (Qingdao, China; approval no. KY202014301).

Patient consent for publication

Not applicable.

Competing interests

The authors declare that they have no competing interests.

References

1. Siegel RL, Miller KD and Jemal A: Cancer statistics, 2020. CA Cancer J Clin 70: 7-30, 2020.
2. DeSantis CE, Ma J, Gaudet MM, Newman LA, Miller KD, Goding Sauer A, Jemal A and Siegel RL: Breast cancer statistics, 2019. CA Cancer J Clin 69: 438-451, 2019.
3. Bishop AJ, Ensor J, Moulder SL, Shaitelman SF, Edson MA, Whitman GJ, Bishnoi S, Hoffman KE, Stauder MC, Valero V, *et al*: Prognosis for patients with metastatic breast cancer who achieve a no-evidence-of-disease status after systemic or local therapy. Cancer 121: 4324-4332, 2015.
4. Liang Y, Zhang H, Song X and Yang Q: Metastatic heterogeneity of breast cancer: Molecular mechanism and potential therapeutic targets. Semin Cancer Biol 60: 14-27, 2020.
5. Bartel DP: MicroRNAs: Target recognition and regulatory functions. Cell 136: 215-233, 2009.
6. Bartel DP: MicroRNAs: Genomics, biogenesis, mechanism, and function. Cell 116: 281-297, 2004.
7. Schmiedel JM, Klemm SL, Zheng Y, Sahay A, Blüthgen N, Marks DS and van Oudenaarden A: Gene expression. MicroRNA control of protein expression noise. Science 348: 128-132, 2015.
8. Loh HY, Norman BP, Lai KS, Rahman N, Alitheen NBM and Osman MA: The regulatory role of MicroRNAs in breast cancer. Int J Mol Sci 20: 4940, 2019.
9. Fan Y, Shi C, Li T and Kuang T: microRNA-454 shows anti-angiogenic and anti-metastatic activity in pancreatic ductal adenocarcinoma by targeting LRP6. Am J Cancer Res 7: 139-147, 2017.
10. Fan Y, Xu LL, Shi CY, Wei W, Wang DS and Cai DF: MicroRNA-454 regulates stromal cell derived factor-1 in the control of the growth of pancreatic ductal adenocarcinoma. Sci Rep 6: 22793, 2016.
11. Li W, Feng Y, Ma Z and Lu L: Expression of miR-454-3p and its effect on proliferation, invasion and metastasis of colon cancer. Nan Fang Yi Ke Da Xue Xue Bao 38: 1421-1426, 2018 (In Chinese).
12. Sun L, Wang Q, Gao X, Shi D, Mi S and Han Q: MicroRNA-454 functions as an oncogene by regulating PTEN in uveal melanoma. FEBS Lett 589: 2791-2796, 2015.
13. Bao X, Ren T, Huang Y, Sun K, Wang S, Liu K, Zheng B and Guo W: Knockdown of long non-coding RNA HOTAIR increases miR-454-3p by targeting Stat3 and Atg12 to inhibit chondrosarcoma growth. Cell Death Dis 8: e2605, 2017.
14. Zuo J, Yu H, Xie P, Liu W, Wang K and Ni H: miR-454-3p exerts tumor-suppressive functions by down-regulation of NFATc2 in glioblastoma. Gene 710: 233-239, 2019.
15. Shao N, Xue L, Wang R, Luo K, Zhi F and Lan Q: miR-454-3p is an exosomal biomarker and functions as a tumor suppressor in glioma. Mol Cancer Ther 18: 459-469, 2019.
16. Fang B, Zhu J, Wang Y, Geng F and Li G: MiR-454 inhibited cell proliferation of human glioblastoma cells by suppressing PDK1 expression. Biomed Pharmacother 75: 148-152, 2015.
17. Li Y, Jiao Y, Fu Z, Luo Z, Su J and Li Y: High miR-454-3p expression predicts poor prognosis in hepatocellular carcinoma. Cancer Manag Res 11: 2795-2802, 2019.
18. Zhou L, Qu YM, Zhao XM and Yue ZD: Involvement of miR-454 overexpression in the poor prognosis of hepatocellular carcinoma. Eur Rev Med Pharmacol Sci 20: 825-829, 2016.
19. Jin C, Lin T and Shan L: Downregulation of Calbindin 1 by miR-454-3p suppresses cell proliferation in nonsmall cell lung cancer in vitro. Cancer Biother Radiopharm 34: 119-127, 2019.
20. Liu S, Ge X, Su L, Zhang A and Mou X: MicroRNA-454 inhibits nonsmall cell lung cancer cells growth and metastasis via targeting signal transducer and activator of transcription-3. Mol Med Rep 17: 3979-3986, 2018.
21. Zhu DY, Li XN, Qi Y, Liu DL, Yang Y, Zhao J, Zhang CY, Wu K and Zhao S: MiR-454 promotes the progression of human non-small cell lung cancer and directly targets PTEN. Biomed Pharmacother 81: 79-85, 2016.
22. Cui X, Xiao D, Cui Y and Wang X: Exosomes-derived long non-coding RNA HOTAIR reduces laryngeal cancer radiosensitivity by regulating microRNA-454-3p/E2F2 axis. Onco Targets Ther 12: 10827-10839, 2019.

23. Wang DY, Li N and Cui YL: Long non-coding RNA CCAT1 sponges miR-454 to promote chemoresistance of ovarian cancer cells to cisplatin by regulation of surviving. Cancer Res Treat 52: 798-814, 2020.
24. Fu Q, Gao Y, Yang F, Mao T, Sun Z, Wang H, Song B and Li X: Suppression of microRNA-454 impedes the proliferation and invasion of prostate cancer cells by promoting N-myc downstream-regulated gene 2 and inhibiting WNT/β-catenin signaling. Biomed Pharmacother 97: 120-127, 2018.
25. Huang C, Liu J, Pan X, Peng C, Xiong B, Feng M and Yang X: miR-454 promotes survival and induces oxaliplatin resistance in gastric carcinoma cells by targeting CYLD. Exp Ther Med 19: 3604-3610, 2020.
26. Jiang D, Li H, Xiang H, Gao M, Yin C, Wang H, Sun Y and Xiong M: Long chain non-coding RNA (lncRNA) HOTAIR knockdown increases miR-454-3p to suppress gastric cancer growth by targeting STAT3/Cyclin D1. Med Sci Monit 25: 1537-1548, 2019.
27. Xu G, Zhu H, Zhang M and Xu J: Histone deacetylase 3 is associated with gastric cancer cell growth via the miR-454-mediated targeting of CHD5. Int J Mol Med 41: 155-163, 2018.
28. Song Z, Li W, Wang L, Jia N and Chen B: MicroRNA-454 inhibits tumor cell proliferation, migration and invasion by downregulating zinc finger Eboxbinding homeobox 1 in gastric cancer. Mol Med Rep 16: 9067-9073, 2017.
29. Song Y, Guo Q, Gao S and Hua K: miR-454-3p promotes proliferation and induces apoptosis in human cervical cancer cells by targeting TRIM3. Biochem Biophys Res Commun 516: 872-879, 2019.
30. Wang S, Zhang G, Zheng W, Xue Q, Wei D, Zheng Y and Yuan J: MiR-454-3p and miR-374b-5p suppress migration and invasion of bladder cancer cells through targetting ZEB2. Biosci Rep 38: BSR20181436, 2018.
31. Guo JY, Wang YK, Lv B and Jin H: miR-454 performs tumor-promoting effects in oral squamous cell carcinoma via reducing NR3C2. J Oral Pathol Med 49: 286-293, 2020.
32. Niu G, Li B, Sun J and Sun L: miR-454 is down-regulated in osteosarcomas and suppresses cell proliferation and invasion by directly targeting c-Met. Cell Prolif 48: 348-355, 2015.
33. Wu X, Ding N, Hu W, He J, Xu S, Pei H, Hua J, Zhou G and Wang J: Down-regulation of BTG1 by miR-454-3p enhances cellular radiosensitivity in renal carcinoma cells. Radiat Oncol 9: 179, 2014.
34. Li X, Hou L, Yin L and Zhao S: LncRNA XIST interacts with miR-454 to inhibit cells proliferation, epithelial mesenchymal transition and induces apoptosis in triple-negative breast cancer. J Biosci 45: 45, 2020.
35. Ren L, Chen H, Song J, Chen X, Lin C, Zhang X, Hou N, Pan J, Zhou Z, Wang L, *et al*: MiR-454-3p-mediated Wnt/β-catenin signaling antagonists suppression promotes breast cancer metastasis. Theranostics 9: 449-465, 2019.
36. Li Q, Liu J, Meng X, Pang R and Li J: MicroRNA-454 may function as an oncogene via targeting AKT in triple negative breast cancer. J Biol Res (Thessalon) 24: 10, 2017.
37. Kalluri R and Weinberg RA: The basics of epithelial-mesenchymal transition. J Clin Invest 119: 1420-1428, 2009.
38. Rastaldi MP: Epithelial-mesenchymal transition and its implications for the development of renal tubulointerstitial fibrosis. J Nephrol 19: 407-412, 2006.
39. Dongre A and Weinberg RA: New insights into the mechanisms of epithelial-mesenchymal transition and implications for cancer. Nat Rev Mol Cell Biol 20: 69-84, 2019.
40. Ding L, Gu H, Xiong X, Ao H, Cao J, Lin W, Yu M, Lin J and Cui Q: MicroRNAs involved in carcinogenesis, prognosis, therapeutic resistance and applications in human triple-negative breast cancer. Cells 8: 1492, 2019.
41. Petri BJ and Klinge CM: Regulation of breast cancer metastasis signaling by miRNAs. Cancer Metastasis Rev 39: 837-886, 2020.
42. Livak KJ and Schmittgen TD: Analysis of relative gene expression data using real-time quantitative PCR and the 2(-Delta Delta C(T)) method. Methods 25: 402-408, 2001.
43. Yang Q, Cao X, Tao G, Zhou F, Zhao P, Shen Y and Chen X: Effects of FOXJ2 on TGF-β1-induced epithelial-mesenchymal transition through Notch signaling pathway in non-small lung cancer. Cell Biol Int 41: 79-83, 2017.
44. Qiang Y, Wang F, Yan S, Zhang H, Zhu L, Chen Z, Tu F, Wang D, Wang G, Wang W and Chen Z: Abnormal expression of Forkhead Box J2 (FOXJ2) suppresses migration and invasion in extrahepatic cholangiocarcinoma and is associated with prognosis. Int J Oncol 46: 2449-2458, 2015.
45. Qiu X, Ji B, Yang L, Huang Q, Shi W, Ding Z, He X, Ban N, Fan S, Zhang J and Tian Y: The role of FoxJ2 in the migration of human glioma cells. Pathol Res Pract 211: 389-397, 2015.
46. Wang Y, Yang S, Ni Q, He S, Zhao Y, Yuan Q, Li C, Chen H, Zhang L, Zou L, *et al*: Overexpression of forkhead box J2 can decrease the migration of breast cancer cells. J Cell Biochem 113: 2729-2737, 2012.
47. Lee C and Huang CH: LASAGNA-Search 2.0: Integrated transcription factor binding site search and visualization in a browser. Bioinformatics 30: 1923-1925, 2014.
48. Crudele F, Bianchi N, Reali E, Galasso M, Agnoletto C and Volinia S: The network of non-coding RNAs and their molecular targets in breast cancer. Mol Cancer 19: 61, 2020.
49. Cao ZG, Li JJ, Yao L, Huang YN, Liu YR, Hu X, Song CG and Shao ZM: High expression of microRNA-454 is associated with poor prognosis in triple-negative breast cancer. Oncotarget 7: 64900-64909, 2016.
50. Jin Y, Liang Z and Lou H: The emerging roles of fox family transcription factors in chromosome replication, organization, and genome stability. Cells 9: 258, 2020.
51. Kehn K, Berro R, Alhaj A, Bottazzi ME, Yeh WI, Klase Z, Van Duyne R, Fu S and Kashanchi F: Functional consequences of cyclin D1/BRCA1 interaction in breast cancer cells. Oncogene 26: 5060-5069, 2007.
52. Qiang Y, Feng L, Wang G, Liu J, Zhang J, Xiang L, Su C, Zhang S, Xie X and Chen E: miR-20a/Foxj2 axis mediates growth and metastasis of colorectal cancer cells as identified by integrated analysis. Med Sci Monit 26: e923559, 2020.
53. Zhang H, Tang QF, Sun MY, Zhang CY, Zhu JY, Shen YL, Zhao B, Shao ZY, Zhang LJ and Zhang H: ARHGAP9 suppresses the migration and invasion of hepatocellular carcinoma cells through up-regulating FOXJ2/E-cadherin. Cell Death Dis 9: 916, 2018.